Electronic Supplementary Information

for

Effects of Structural Modification of (Alkyldiene-Imidazolium Bromide)-Based Gemini Monomers on the Formation of the Lyotropic Bicontinuous Cubic Phase

Patrick Li,[a] Maria I. Reinhardt,[a] Samantha S. Dyer,[a] Kara E. Moore,[a] Omar Q. Imran[b, c] and Douglas L. Gin*[, a]

[a]*Department of Chemistry, University of Colorado, Boulder, CO 80309, USA.*

[b]*Department of Chemical and Environmental Engineering, Yale University, New Haven, CT 06510, USA*

[c]*Department of Chemical and biomolecular Engineering, University of Pennsylvania, Pennsylvania, PA 19104, USA.*

Instruments and Materials

NMR spectra were obtained using a Bruker Avance-III 300 NMR spectrometer (300 MHz for ^{1}H, 75 MHz for ^{13}C). Chemical shifts are reported in parts per million relative to the solvent residual signal ($CDCl_3$, δ_H = 7.26 ppm, δ_C = 77.16 ppm; DMSO-d_6, δ_H = 2.50 ppm, δ_C = 39.52 ppm). IR spectra (neat) were recorded using a Thermo Scientific Nicolet 6700 FT-IR equipped with a Pike MIRacle^{TM} single-reflection horizontal attenuated total reflectance accessory. Lyotropic liquid-crystalline (LLC) mixtures were homogenized, as needed, using an IEC Centra-CL2 centrifuge. Elemental analysis was performed by Galbraith Laboratories, Inc. Powder X-ray diffraction (PXRD) was the primary quantitative phase identification method used: PXRD spectra were obtained using an Inel CPS 120 diffraction system at the University of Colorado Boulder

using a monochromated Cu K_α radiation source. This apparatus was equipped with a rotating flat, circular aluminum sample pan and a custom-built programmable sample heating stage for variable-temperature PXRD (VT-PXRD) of powder or spreadable samples using a conventional powder diffraction geometry. In addition, the PXRD instrument was equipped with a custom-made, sandwich-type, aluminum film holder with an open central window that allowed X-ray diffraction analysis of film samples by positioning the open face of the sample film directly in the path of the X-ray beam, between the beam source and the detector (i.e., through-film transmission mode). For both flat-pan PXRD or through-film configurations, all PXRD spectra were calibrated against a silver behenate diffraction standard (d_{100} = 58.4 Å) loaded in the same sample configuration and using the appropriate diffraction geometry as described for each method.[1] In the case of the through-film transmission configuration, the silver behenate powder was sandwiched between Mylar sheets before placing in the film holder apparatus. To help confirm/verify the Q phase information provided by PXRD, small-angle X-ray scattering (SAXS) was performed on a single sample previously analyzed by PXRD by collaborators at the University of Pennsylvania as a special one-time, non-routine request. SAXS spectra were measured using a Xenocs Xeuss 2.0 system in the Dual Source and Environmental X-ray Scattering (DEXS) facility at the University of Pennsylvania. A GeniX3D Cu source with a wavelength of λ = 1.54 Å was used, with a typical sample-to-detector distance of 37.5 cm, providing a range of accessible scattering vectors (q) from 0.016 to 1.4 $Å^{-1}$. Silver behenate was used as a standard for calibrating the SAXS sample-to-detector distance, and film samples were packed between Kapton windows. Foxtrot software was used for azimuthal integration of scattering patterns into 1-D plots of scattering intensity (I) vs. q, where $q = 4\pi\sin(\theta)/\lambda$ and the scattering angle is 2θ. Variable-temperature polarized light microscopy (PLM) studies were performed using a Leica DMRXP polarizing light microscope

equipped with a Q-Imaging MicroPublisher 3.3 RTV digital camera, a Linkam LTS 350 thermal stage, and a Linkam CI 94 temperature controller. Automatic temperature profiles and image captures were performed using Linkam Linksys32 software. Radical photopolymerizations were conducted using a Spectroline XX-15A 365 nm UV lamp (8.5 mW/cm^2 at the sample surface). UV light fluxes at the sample surface were measured using a Spectroline DCR-100X digital radiometer equipped with a DIX-365 UV-A sensor.

Chromium (IV) oxide, pyridine, *tert*-butyllithium (1.6 M in pentane), hydrogen bromide (48 wt. % in H_2O), borane-tetrahydrofuran complex solution (1.0 M in THF), sodium hydride (60 wt. % dispersion in mineral oil), imidazole, ω-pentadecalactone (98%), 2-hydroxy-2-methylpropiophenone (HMP, 97%), sulfuric acid, 1,4-dibromobutane (99%), 1,6-dibromohexane (96%), triethanolamine (98%), and Florisil® (<200 mesh) were purchased from the Sigma-Aldrich Chemical Co. and used as received unless otherwise specified. 11-Bromo-1-undecanol (97%), 1,5-dibromopentane (98%), 1,7-dibromoheptane (98%), 1,9-dibromononane (97%), *N,N,N',N'*,-tetramethylethylenediamine (98%), allyltrimethylsilane (98%), and 2-isopropoxy-4,4,5,5-tetramethyl-1,3,2-dioxaborolane (98%) were purchased from TCI America and used as received unless otherwise specified. Aluminum oxide (neutral, act. I, 50-200 μm) and silica gel (normal-phase, 200 x 400 mesh) were purchased from Sorbent Technologies. Glycerol (ACS Reagent) was purchased from Mallinckrodt and used as received. Sodium hydroxide, sodium chloride, magnesium sulfate, Celite™ 545, and hydrochloric acid (all ACS Reagents) were purchased from Fisher Scientific and used as received. All reaction solvents were obtained from the Sigma-Aldrich Chemical Co. and were purified/dehydrated via vacuum distillation and then de-gassed by repeated freeze-pump-thaw cycles and stored under Ar. All chemical syntheses were carried out under a dry Ar atmosphere using standard Schlenk line techniques unless otherwise noted.

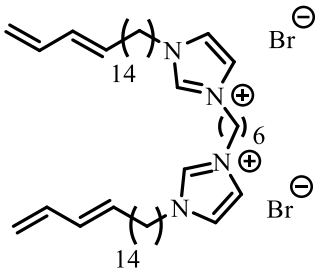

1

Fig. S1 Structure of gemini LLC monomer **1**.

New LLC monomer synthesis and characterization.

The seven homologues of Q_I-phase-forming monomer **1** (Fig. S1),[2] were prepared as shown in Fig. S2 below. Detailed synthesis and structural characterization information on each of these new monomers are listed below. The newly synthesized homologues are hygroscopic, ionic organic compounds that are difficult to dry completely and usually do not combust well. However, their obtained elemental analysis values are within the accepted ±0.4% tolerance range for C, H, and N to be considered pure when the presence of associated water molecules is accounted for (as for prior monomer **1**).[3] To help verify the purities of the new homologues, example ^{1}H and ^{13}C NMR spectra of some of the final monomers have also been included at the end of the ESI to show the lack of impurities other than associated water.

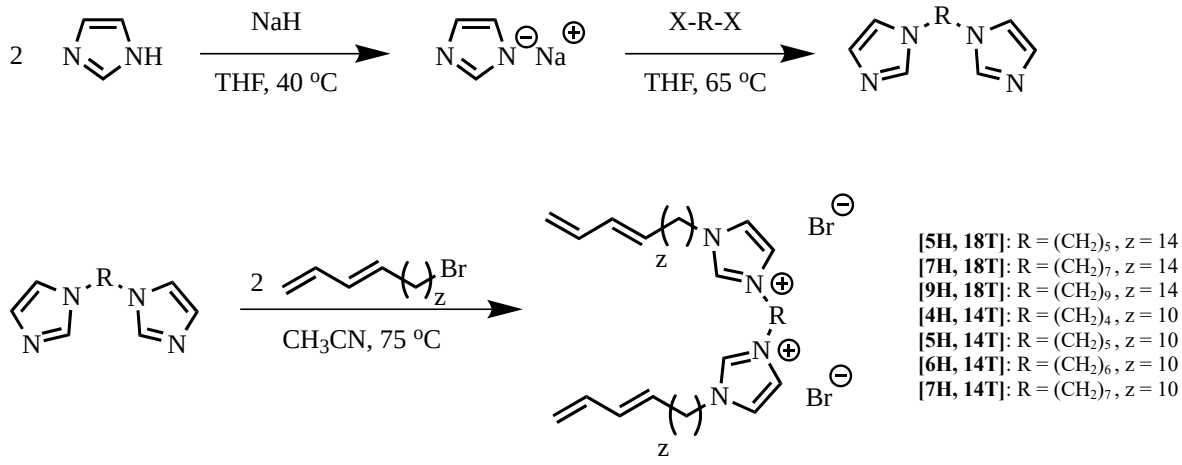

Fig. S2 General synthetic scheme for the seven monomer **1** homologues that were tested for Q-phase formation in the presence of glycerol and water.

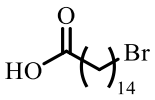

15-Bromopentadecanoic acid.[4] ω-Pentadecalactone (50.00 g, 0.2080 mol, 1.000 equiv.) was stirred in 48 wt. % aq. HBr (295.2 mL, 2.610 mol, 12.55 equiv.) in a 500-mL round-bottom flask equipped with a stir bar and reflux condenser. Conc. H_2SO_4 (33.26 mL, 0.6240 mol, 3.000 equiv.) was added dropwise to minimize exothermic activity, liquefying the solid lactone. The solution was heated to 120 °C and stirred for 84 h. The solution was cooled to room temperature and then decanted, leaving a black solid disc behind in the round-bottom flask. The disc was rinsed with de-ionized (DI) H_2O (2 x 200 mL), and the rinse was discarded. CH_2Cl_2 (300 mL) was then added to the flask, and the solution was heated to 35 °C and stirred until the black disc was completely dissolved. The resulting organic solution was filtered through a pad of Celite™ 545. The resulting filtrate was washed with DI H_2O (2 x 200 mL), brine (2 x 200 mL), and DI H_2O again (2 x 200 mL). The black film that formed between the organic and aqueous phases was discarded, and the

organic phase was then dried over anhydrous $MgSO_4$. The resulting organic solution was reduced by rotary evaporation to afford an off-white, crystalline solid (54.85 g, 82%). Spectroscopic characterization and purity data for this compound matched published data.[4]

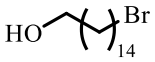

15-Bromopentadecanol.[4] Borane-THF complex solution (234.0 mL, 0.2340 mol, 1.504 equiv.) was cannula transferred under Ar into a 500-mL three-neck round-bottom flask equipped with a stir bar. 15-Bromopentadecanoic acid (50.00 g, 0.1556 mol, 1.000 equiv.) was added slowly at 0 °C to minimize bubbling. The light-yellow solution was warmed to room temperature and then stirred under Ar for 24 h. The reaction solution was then quenched with DI H_2O (200 mL) followed by 1.2 M aq. HCl (15.00 mL). The resulting mixture was then extracted with Et_2O (2 x 150 mL) and washed with brine (3 x 250 mL). The organic phase was then dried over anhydrous $MgSO_4$. The resulting organic solution was reduced by rotary evaporation to afford an off-white, powder. The resulting powder was recrystallized from hot MeOH and washed with cold MeOH to afford the product as a white, crystalline solid (40.27 g, 84%). Spectroscopic characterization and purity data for this compound matched published data.[4]

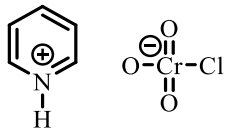

Pyridinium chlorochromate (PCC) on alumina.[5]

The following procedure was performed in air with materials used as purchased. 6 M Aq. HCl (111.7 mL, 0.6701 mol, 1.340 equiv.) was added to a 1-L round-bottom flask and stirred. Chromium (VI) oxide (50.00 g, 0.5001 mol, 1.000 equiv.) was added slowly and the reaction

mixture was cooled in an ice bath. Anhydrous pyridine (40.45 mL, 0.5001 mol, 1.000 equiv.) was then added slowly. The orange reaction slurry was raised to 45 °C and stirred until the mixture became a homogeneous liquid. The reaction mixture was then removed from heat, and alumina (neutral, act. I, 50–200 μm, 368 g) was added slowly. The resulting mixture was manually stirred until all the alumina was uniformly coated. The mixture was then dried in air overnight at ambient temperature, and then dried in vacuo at ambient temperature to give the product as a bright orange powder (476.2 g, 1.050 x 10^{-3} mol PCC/g, 100%).

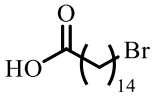

15-Bromopentadecanal.[4] PCC on alumina (55.78 g, 0.05850 mol, 1.800 equiv.) was added to a 500 mL three-neck round-bottom flask equipped with a stir bar. CH_2Cl_2 (300 mL, not anhydrous) was added to the reaction flask and the solution was stirred at a moderate speed. 15-Bromopentadecanol (10.00 g, 0.03250 mol, 1.000 equiv.) was added and the reaction flask was stoppered with a rubber septum with a venting needle. The needle was removed after 1 h, and the reaction slurry was stirred vigorously for 12 h. The reaction slurry was passed through a 150-mL fritted funnel filled with 0.5 cm of silica gel, 2 cm of Florisil®, and another 0.5 cm of silica gel with additional CH_2Cl_2 (400 mL). Concentration of the CH_2Cl_2 under rotary evaporation afforded the product as a white solid (9.62 g, 97%). Spectroscopic characterization and purity data for this compound matched published data.[4]

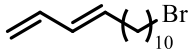

14-Bromotetradeca-1,3-diene.[6] This compound was synthesized as described in the literature.[6] Spectroscopic characterization and purity data for this compound matched published data.[6]

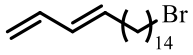

18-Bromooctadeca-1,3-diene.[6] This compound was synthesized as described in the literature.[6] Spectroscopic characterization and purity data for this compound matched published data.[6]

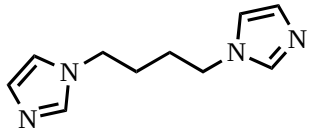

1,1'-(1,4-Butanediyl)bisimidazole.[2] 60 wt. % Sodium hydride in mineral oil (1.711 g, 0.04278 mol, 2.800 equiv.) and THF (150 mL) were added to a 250 mL, three-neck, round-bottom flask equipped with a reflux condenser and stir bar. The slurry was cooled to 0 °C, and imidazole (2.289 g, 0.03362 mol, 2.200 equiv.) was added slowly. The resulting mixture was heated at 40 °C for 15 min. 1,4-Dibromobutane (3.300 g, 0.01528 mol, 1.000 equiv.) was then injected, and the reaction mixture was stirred at 65 °C for 12 h. The contents of the flask were filtered and washed with additional THF (50 mL). The filtrate was concentrated under rotary evaporation to afford a yellow-orange oil. The resulting oil was dissolved in CH_2Cl_2 (100 mL), extracted with 1.2 M aq. HCl (100 mL), and washed with CH_2Cl_2 (3 x 100 mL). 1 M Aq. NaOH was added to the aqueous layer until a pH of 8 was achieved, and this aqueous solution was then extracted with CH_2Cl_2 (3 x 100 mL). The combined CH_2Cl_2 extracts were dried over anhydrous $MgSO_4$ and then concentrated by rotary evaporation to afford the product as a white solid (1.4195 g, 49%). Spectroscopic characterization and purity data for this compound matched published data.[2]

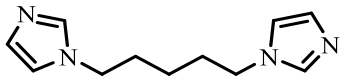

1,1'-(1,5-Pentanediyl)bisimidazole.[7] This compound was synthesized as described in the literature.[7] Spectroscopic characterization and purity data for this compound matched published data.[7]

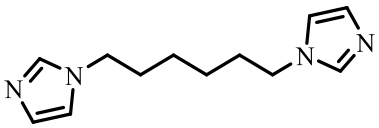

1,1'-(1,6-Hexanediyl)bisimidazole.[8] This compound was synthesized as described in the literature.[8] Spectroscopic characterization and purity data for this compound matched published data.[8]

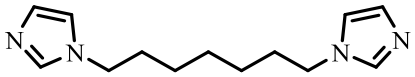

1,1'-(1,7-Heptanediyl)bisimidazole.[7] This compound was synthesized in a similar way as 1,1'-(1,4-butanediyl)bisimidazole but using 1,7-dibromoheptane instead of 1,4-dibromobutane. Spectroscopic characterization and purity data for this compound matched published data.[7]

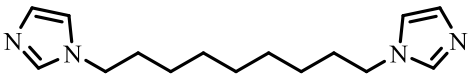

1,1'-(1,9-Nonanediyl)bisimidazole.[9] This compound was synthesized in a similar way as 1,1'-(1,4-butanediyl)bisimidazole but using 1,9-dibromononane instead of 1,4-dibromobutane. Spectroscopic characterization and purity data for this compound matched published data.[9]

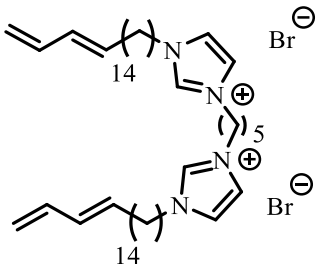

1,5-Bis(octadeca-15,17-dienylimidazolium)pentane dibromide [5H, 18T]. 18-Bromooctadeca-1,3-diene (1.04 g, 3.16 mmol, 2.31 equiv.) and 1,1'-(1,5-pentanediyl)bisimidazole (0.29 g, 1.4 mmol, 1.0 equiv.) were dissolved in CH_3CN (15 mL) in a 15-mL Schlenk flask equipped with a stir bar. The solution was stirred at 75 °C for 72 h in the dark. The contents of the Schlenk flask were cooled to room temperature, transferred to a 250-mL round-bottom flask equipped with a stir bar, and precipitated from Et_2O (200 mL). The resulting mixture was stirred at room temperature for 30 min, filtered, washed with additional Et_2O (100 mL), and dried in vacuo to give **[5H, 18T]** as a white solid (1.10 g, 93%). ^{1}H NMR (300 MHz, DMSO-d_6): δ 9.30 (t, J = 1.6 Hz, 1H), 7.82 (dd, J = 1.6, 0.6 Hz, 2H), 6.35 – 6.19 (m, 1H), 6.15 – 5.94 (m, 1H), 5.81 – 5.63 (m, 1H), 5.14 – 4.88 (m, 2H), 4.17 (q, J = 6.9 Hz, 4H), 2.03 (t, J = 7.0 Hz, 2H), 1.81 (dt, J = 14.8, 7.4 Hz, 4H), 1.41 – 1.13 (m, 24H). ^{13}C NMR (75 MHz, DMSO-d_6): δ 137.21, 135.97, 135.26, 130.86, 122.44, 115.07, 48.84, 48.43, 31.87, 29.33, 29.02, 28.98, 28.95, 28.84, 28.60, 28.57, 28.36, 25.51. FTIR (neat): 3057, 2918, 2850, 1565, 1463, 1162, 1012, 1001, 916, 835, 723 cm^{-1}. Calc. for $C_{47}H_{82}Br_2N_4$: C, 65.41; H, 9.58; N, 6.49. Calc. for $C_{47}H_{82}Br_2N_4 \bullet 0.5H_2O$: C, 64.74; H, 9.59; N, 6.43. Found: C, 64.65; H, 9.29; N, 6.37.

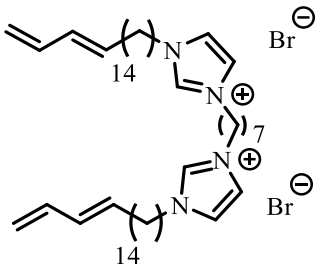

1,7-Bis(octadeca-15,17-dienylimidazolium)heptane dibromide [7H, 18T]. 18-Bromooctadeca-1,3-diene (1.02 g, 3.10 mmol, 2.30 equiv.) and 1,1'-(1,7-heptanediyl)bisimidazole (0.313 g, 1.35 mmol, 1.00 equiv.) were dissolved in CH_3CN (15 mL) in a 15-mL Schlenk flask equipped with a stir bar. The solution was stirred at 75 °C for 72 h in the dark. The contents of the Schlenk flask were cooled to room temperature, transferred to a 250-mL round-bottom flask equipped with a stir bar, and precipitated from Et_2O (200 mL). The resulting mixture was stirred at room temperature for 30 min, filtered, washed with additional Et_2O (100 mL), and dried in vacuo to give **[7H, 18T]** as a white solid (1.12 g, 93%). ^{1}H NMR (300 MHz, DMSO-d_6): δ 9.30 (s, 2H), 7.82 (d, J = 1.6 Hz, 4H), 6.41 – 6.15 (m, 2H), 6.12 – 5.92 (m, 2H), 5.82 – 5.61 (m, 2H), 5.15 – 4.86 (m, 4H), 4.16 (t, J = 7.2 Hz, 8H), 2.04 (q, J = 6.7 Hz, 4H), 1.78 (p, J = 7.3 Hz, 8H), 1.47 – 1.08 (m, 53H). ^{13}C NMR (75 MHz, DMSO-d_6): δ 137.20, 135.93, 135.26, 130.86, 122.44, 115.06, 48.81, 48.73, 31.87, 29.28, 29.18, 29.02, 28.98, 28.92, 28.83, 28.59, 28.57, 28.32, 25.47, 25.29. FTIR (neat): 2981, 2917, 2850, 1561, 1467, 1164, 1002, 949, 916, 820, 721 cm^{-1}. Calc. for $C_{49}H_{86}Br_2N_4$: C, 66.05; H, 9.73; N, 6.29. Calc. for $C_{49}H_{86}Br_2N_4 \cdot 0.5H_2O$: C, 65.39; H, 9.74; N, 6.22. Found: C, 65.55; H, 10.06; N, 6.30.

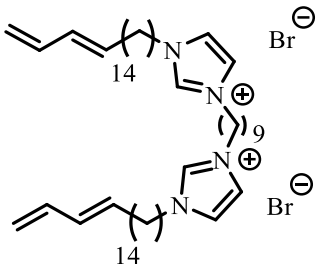

1,9-Bis(octadeca-15,17-dienylimidazolium)nonane dibromide [9H, 18T]. 18-Bromooctadeca-1,3-diene (1.25 g, 3.80 mol, 2.30 equiv.) and 1,1'-(1,9-nonanediyl)bisimidazole (0.43 g, 1.7 mol, 1.0 equiv.) were dissolved in CH_3CN (15 mL) in a 15-mL Schlenk flask equipped with a stir bar. The solution was stirred at 75 °C for 72 h in the dark. The contents of the Schlenk flask were cooled to room temperature, transferred to a 250-mL round-bottom flask equipped with a stir bar, and precipitated from Et_2O (200 mL). The resulting mixture was stirred at room temperature for 30 min, filtered, washed with additional Et_2O (100 mL), and dried in vacuo to give **[9H, 18T]** as a white solid (1.31 g, 86%). ^{1}H NMR (300 MHz, DMSO-d_6): δ 9.29 (t, J = 1.6 Hz, 2H), 7.82 (d, J = 1.6 Hz, 4H), 6.41 – 6.15 (m, 2H), 6.17 – 5.92 (m, 2H), 5.82 – 5.63 (m, 2H), 5.13 – 4.91 (m, 4H), 4.16 (t, J = 7.1 Hz, 8H), 2.04 (q, J = 6.7 Hz, 4H), 1.78 (p, J = 7.3 Hz, 8H), 1.41 – 1.10 (m, 56H). ^{13}C NMR (75 MHz, DMSO-d_6): δ 137.20, 135.94, 135.25, 130.86, 122.45, 115.06, 48.80, 31.87, 29.29, 29.26, 29.01, 28.98, 28.90, 28.83, 28.59, 28.57, 28.31, 28.28, 25.47, 25.44. FTIR (neat): 2918, 2850, 1561, 1467, 1165, 1003, 949, 919, 836, 746, 721 cm^{-1}. Calc. for $C_{51}H_{90}Br_2N_4$: C, 66.65; H, 9.87; N, 6.10. Calc. for $C_{51}H_{90}Br_2N_4 \cdot 1.5H_2O$: C, 64.74; H, 9.91; N, 5.92. Found: C, 64.70; H, 9.57; N, 5.90.

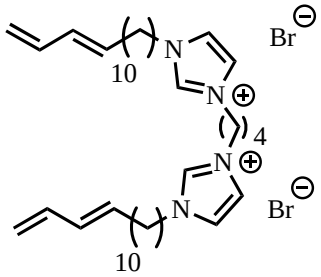

1,4-Bis(tetradeca-11,13-dienylimidazolium)butane dibromide [4H, 14T].[2] This compound was synthesized in a similar way as 1,5-bis(octadeca-15,17-dienylimidazolium)pentane dibromide but using 1,1'-(1,4-butanediyl)bisimidazole instead of 1,1'-(1,5-pentanediyl)bisimidazole and 14-bromotetradeca-1,3-diene instead of 18-bromooctadeca-1,3-diene. Spectroscopic characterization and purity data for this compound matched published data.[2]

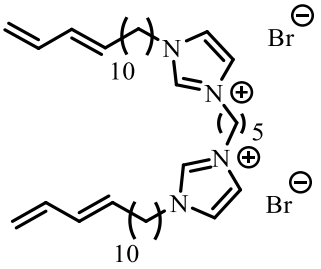

1,5-Bis(tetradeca-11,13-dienylimidazolium)pentane dibromide [5H, 14T]. 14-Bromotetradeca-1,3-diene (1.46 g, 5.34 mmol, 2.27 equiv.) and 1,1'-(1,5-pentanediyl)bisimidazole (0.47 g, 2.4 mmol, 1.0 equiv.) were dissolved in CH_3CN (15 mL) in a 15-mL Schlenk flask equipped with a stir bar. The solution was stirred at 75 °C for 72 h in the dark. The contents of the Schlenk flask were cooled to room temperature, transferred to a 250-mL round-bottom flask equipped with a stir bar, and precipitated from Et_2O (200 mL). The resulting mixture was stirred at room temperature for 30 min, filtered, washed with additional Et_2O (100 mL), and dried in vacuo to give **[5H, 14T]** as a white solid (1.60 g, 91%). ^{1}H NMR (300 MHz, DMSO-d_6): δ 9.32 (t, J = 1.6 Hz, 2H), 7.83 (p, J = 1.9 Hz, 4H), 6.40 – 6.18 (m, 2H), 6.12 – 5.94

(m, 2H), 5.79 – 5.59 (m, 2H), 5.13 – 4.87 (m, 4H), 4.18 (q, J = 7.0 Hz, 8H), 2.04 (q, J = 6.7 Hz, 4H), 1.81 (dp, J = 14.3, 7.1 Hz, 8H), 1.50 – 1.15 (m, 32H). ^{13}C NMR (75 MHz, DMSO-d_6): δ 137.20, 135.98, 135.25, 130.87, 122.44, 115.09, 48.83, 48.42, 31.87, 29.32, 28.87, 28.80, 28.60, 28.57, 28.33, 25.50, 22.02. FTIR (neat): 3054, 2919, 2852, 1564, 1462, 1161, 1012, 1002, 916, 831, 749, 723 cm^{-1}. Calc. for $C_{39}H_{66}Br_2N_4$: C, 62.39; H, 8.86; N, 7.46. Calc. for $C_{39}H_{66}Br_2N_4 \cdot 1.5H_2O$: C, 60.22; H, 8.94; N, 7.20. Found: C, 60.23; H, 8.74; N, 7.18.

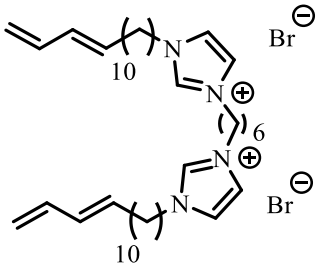

1,6-Bis(tetradeca-11,13-dienylimidazolium)hexane dibromide [6H, 14T].[2] This compound was synthesized in a similar way as 1,5-bis(octadeca-15,17-dienylimidazolium)pentane dibromide but using 1,1'-(1,6-hexanediyl)bisimidazole instead of 1,1'-(1,5-pentanediyl)bisimidazole and 14-bromotetradeca-1,3-diene instead of 18-bromooctadeca-1,3-diene. Spectroscopic characterization and purity data for this compound matched published data.[2]

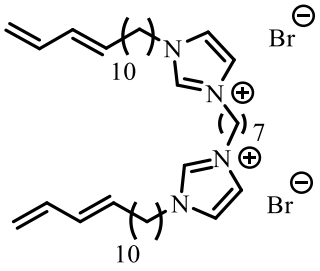

1,7-Bis(tetradeca-11,13-dienylimidazolium)heptane dibromide [7H, 14T]. 14-Bromotetradeca-1,3-diene (1.62 g, 5.93 mmol, 2.30 equiv.) and 1,1'-(1,7-

heptanediyl)bisimidazole (0.60 g, 2.6 mmol, 1.0 equiv.) were dissolved in CH_3CN (15 mL) in a 15-mL Schlenk flask equipped with a stir bar. The solution was stirred at 75 °C for 72 h in the dark. The contents of the Schlenk flask were cooled to room temperature, transferred to a 250-mL round-bottom flask equipped with a stir bar, and precipitated from Et_2O (200 mL). The resulting mixture was stirred at room temperature for 30 min, filtered, washed with additional Et_2O (100 mL), and dried in vacuo to give **[7H, 14T]** as a white solid (1.41 g, 70%). ^1H NMR (300 MHz, DMSO-d_6): δ 9.23 (t, J = 1.6 Hz, 2H), 7.85 – 7.64 (m, 4H), 6.45 – 6.14 (m, 2H), 6.11 – 5.90 (m, 2H), 5.81 – 5.57 (m, 2H), 5.14 – 4.90 (m, 4H), 4.15 (t, J = 7.2 Hz, 8H), 2.04 (q, J = 7.0 Hz, 4H), 1.79 (q, J = 7.2 Hz, 8H), 1.51 – 1.02 (m, 37H). ^{13}C NMR (75 MHz, DMSO-d_6): δ 137.21, 135.92, 135.26, 130.88, 122.45, 115.11, 48.83, 48.75, 31.88, 29.28, 29.20, 28.85, 28.81, 28.79, 28.61, 28.58, 28.30, 27.69, 25.46, 25.31. FTIR (neat): 3068, 2923, 2853, 1562, 1461, 1162, 1022, 972, 842, 724 cm^{-1}. Calc. for $C_{41}H_{70}Br_2N_4$: C, 63.23; H, 9.06; N, 7.19. Calc. for $C_{41}H_{70}Br_2N_4 \bullet 0.5H_2O$: C, 62.51; H, 9.08; N, 7.11. Found: C, 62.24; H, 9.15; N, 7.10.

Qualitative screening of LLC phase behaviour and potential Q phase formation with different solvents using the PLM-based penetration scan technique.[10c]

To quickly and qualitatively determine the LLC phase behaviour of homologues of monomer **1** (see Table S1) with a specific added solvent, the PLM penetration scan technique was employed.[10c] This technique is a solvent-amphiphile gradient assay using PLM that quickly (i.e., in minutes) determines qualitatively what phases can be formed by a certain amphiphile and solvent pair at a specific temperature. This technique was performed by taking the solid monomer and pressing it between a microscope slide and a cover slip. The sample was then placed on the

PLM thermal stage and annealed to its melting temperature or up to 90 °C, whichever came first. The sample was then slowly cooled back down to room temperature. A small amount (<30 μL) of the chosen solvent was added to the edge of the cover slip, and the solvent was drawn via capillary action into contact with the solid monomer, creating a concentration gradient. The specimen was then heated to 95 °C at a rate of 5 °C/min on the PLM programmable hot/cold stage, and its optical texture under crossed polarizers as a function of temperature was recorded via digital image capture. The differences in optical texture were used to determine the potential LLC phases formed. Since Q phases are black (i.e., isotropic) under PLM and are typically found between birefringent lamellar (L) and hexagonal (H) phases, a dark isotropic band between two birefringent LLC phases indicates a potential Q phase.[10c] The seven homologues of monomer **1** were evaluated in this fashion with glycerol and with water.

Table S1. Summary of the preliminary qualitative Q-phase formation behaviour of monomer **1** and its seven homologues studied in this work when mixed with glycerol and water in the 25–95 °C temperature range, as determined via PLM-based solvent-penetration scan screening studies. These results do not guarantee the presence of a Q phase without more detailed phase diagram analysis of carefully prepared mixtures via full PLM phase elucidation supported by PXRD confirmation.

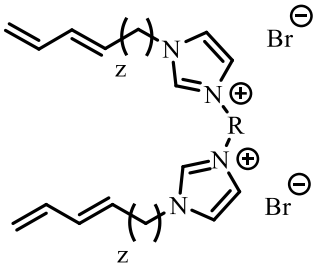

			Potential Q Phase via Penetration Scan		Potential Q Phase Onset Temperature (°C)	
Monomer	**R**	**z**	**Glycerol**	**Water**	**Glycerol**	**Water**
1	6	14	Yes	Yes	65	68
[5H, 18T]	5	14	Yes	Yes	46	58
[7H, 18T]	7	14	Yes	Yes	51	48
[9H, 18T]	9	14	Yes	Yes	40	43
[4H, 14T]	4	10	No	Yes	(not applicable)	40
[5H, 14T]	5	10	Yes	Yes	25	26
[6H, 14T]	6	10	No	Yes	(not applicable)	29
[7H, 14T]	7	10	No	No	(not applicable)	(not applicable)

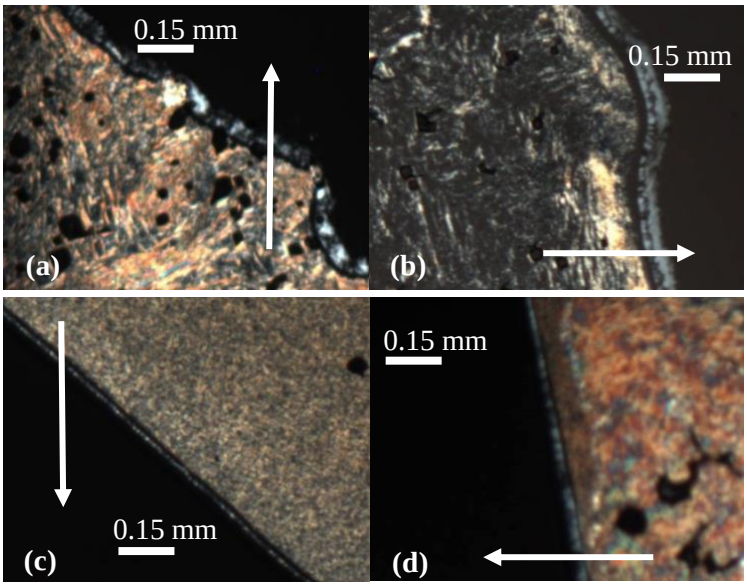

Fig. S3 Representative PLM images (magnification: 50x) of glycerol penetration scans of homologues **[5H, 18T]**, **[7H, 18T]**, **[9H, 18T]**, and **[5H, 14T]**: (a) potential Q-phase formation for **[5H, 18T]** at 46 °C; (b) potential Q-phase formation for **[7H, 18T]** at 51 °C; (c) potential Q-phase formation for **[9H, 18T]** at 40 °C; (d) potential Q phase formation for **[5H, 14T]** at 25 °C. The black (pseudo-isotropic region) between two bright, anisotropic LLC regions is indicative of the presence of a potential Q phase.[10c] The arrows in the PLM images point in the direction of increasing glycerol concentration.

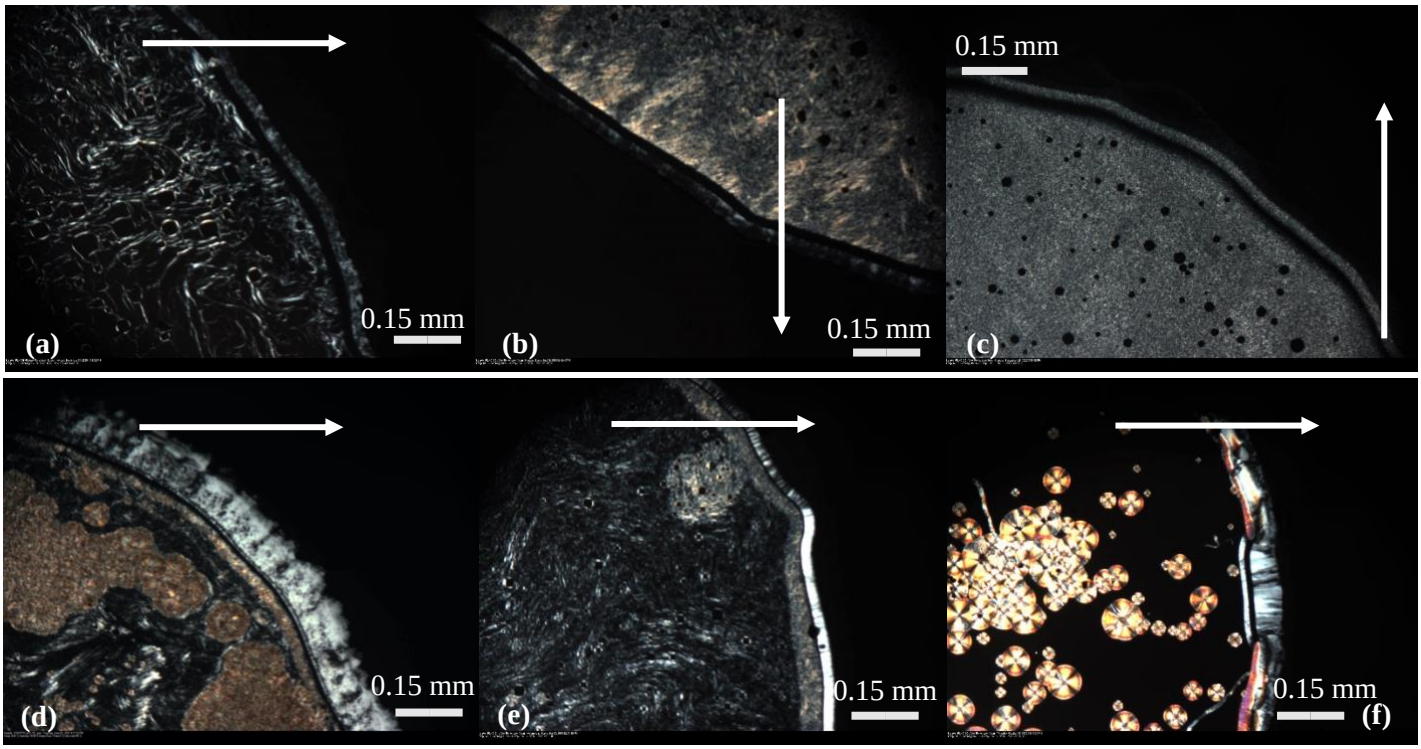

Fig. S4 Representative PLM images (magnification: 50x) of water penetration scans of homologues **[5H, 18T]**, **[7H, 18T]**, **[9H, 18T]**, **[4H, 14T]**, **[5H, 14T]**, and **[6H, 14T]**: (a) potential Q-phase formation for monomer **[5H, 18T]** at 58 °C; (b) potential Q-phase formation for monomer **[7H, 18T]** at 48 °C; (c) potential Q-phase formation in monomer **[9H, 18T]** at 43 °C; (d) potential Q-phase formation for monomer **[4H, 14T]** at 40 °C, (e) potential Q phase formation for monomer **[5H, 14T]** at 26 °C; (f) potential Q-phase formation in monomer **[6H, 14T]** at 29 °C. The black (pseudo-isotropic region) between two bright, anisotropic LLC regions is indicative of the presence of a potential Q phase.[10c] The arrows in the PLM images point in the direction of increasing water concentration.

Preparation of LLC samples, determination of LLC phase behaviour, and elucidation of partial phase diagrams.

LLC samples of specific composition were made by adding an appropriate amount of monomer and solvent to custom-made glass vials. A small amount (i.e., 1 wt. % of the total mixture mass) of radical photo-initiator, 2-hydroxy-2-methylpropiophenone (HMP), was added if required; and the vials were sealed with Parafilm™. LLC samples were mixed by alternately hand-mixing and centrifuging (2800 rpm) until completely homogeneous. It should be noted that the LLC samples are sensitive to water loss or gain, depending on the solvent system. Special attention was taken to keep the samples sealed as much as possible during sample mixing and transferring to minimize composition drift.

For samples prepared with water, LLC samples of specific composition were prepared by adding the desired mass of monomer to tared, custom-made glass vials placed on a microbalance, followed by the addition of an appropriate mass of solvent via pipette. HMP photo-initiator (1 wt. % of the total mixture mass) was then added if required. The vials were sealed with Parafilm™ and centrifuged at 2800 rpm. The samples were then alternately hand-mixed and centrifuged (2800 rpm) until homogeneous by visual inspection (ca. three cycles of hand-mixing and centrifuging).

For samples prepared with glycerol, LLC samples of specific composition were prepared by adding the desired mass of solvent to tared, custom-made glass vials placed on a microbalance, followed by the addition of an appropriate mass of monomer via spatula. HMP photo-initiator (1 wt. % of the total mixture mass) was then added if required. The vials were sealed with Parafilm™ and centrifuged at 2800 rpm. The samples were then alternately hand-mixed and centrifuged (2800) until homogeneous by visual inspection (ca. three cycles of hand-mixing and centrifuging).

The composition and temperature ranges of the LLC phases formed by the mixtures described above were determined using variable-temperature PLM. Specimens of various mixture compositions were prepared and then pressed between a microscope slide and microscope cover-slip to help minimize composition drift from ambient atmospheric water uptake or solvent evaporation. This assembly was then placed on the PLM programmable hot/cold stage and annealed past its isotropic temperature or up to 90 °C (whichever came first). The sample was slowly cooled and allowed to come back to its room-temperature phase. The sample was then heated to 95 °C at a rate of 5 °C/min, and its optical textures as a function of temperature were recorded via digital image capture. Images were captured at 50x magnification. Changes in optical texture were used to determine changes in the LLC phase of the mixture.

Whenever possible, the identity of each observed phase was confirmed using ambient-temperature PXRD by analyzing a bulk film of a composition point in each distinct phase region (as elucidated by PLM analysis) that was photo-cross-linked to permanently trap the phase microstructure. A sample with radical photo-initiator was placed between Mylar sheets with a thickness-appropriate spacer (to minimize composition drift due to ambient atmospheric water uptake or solvent evaporation), annealed at the appropriate temperature for 15 min on a programmable hot plate, and then photopolymerized for 1 h while held at that temperature. Room-temperature PXRD spectra of the resulting cross-linked bulk film samples were taken in the open air using a custom-made, clamped sandwich-type film holder with a central open window. The clamped polymer film was then positioned such that the open face of the film was directly in the path of the X-ray beam, between the beam source and the detector (i.e., through-film transmission mode). The *d*-spacing pattern of the PXRD peaks was used to quantitatively identify the type of LLC phase formed at the specified composition and temperature used to form the cross-linked

sample, so long as more than one PXRD peak are present to clearly index an LLC phase with a specific geometry.[10]

Variable-temperature PXRD (VT-PXRD) analysis of unpolymerized LLC mixtures for phase identification was used to check non-Q-phase boundaries or if ambient-temperature PXRD analysis of a bulk film was not informative enough to draw conclusions on the phase. An LLC mixture of a composition point in each distinct region was formulated as described above but without photo-initiator. The (LLC monomer + glycerol or water) mixture was then spread onto the top of an open-face, circular aluminum pan (approx. sample dimensions: 10 mm in diameter x 0.2 mm thick), which was placed on a custom-built programmable sample heating stage for the PXRD instrument. The top of the unpolymerized mixture in the sample pan was then covered with a piece of Mylar sheet to minimize composition drift due to ambient water uptake or solvent evaporation, and allowed to equilibrate for 5–10 min. The Mylar-film-covered, unpolymerized sample then was analyzed via PXRD using a conventional powder diffraction geometry while held at the desired temperature for 1–2 h. The *d*-spacing pattern of the PXRD peaks was used to quantitatively identify the type of LLC phase formed, so long as more than one diffraction peak are present to clearly index an LLC phase with a specific geometry.[10] In the event that both ambient-temperature PXRD and VT-PXRD were not informative enough to draw conclusions on a suspected Q-phase region, bulk film samples were sent off to our collaborators at the University of Pennsylvania for SAXS analysis.

For illustration purposes, a schematic representation of the various phase regions and the different LLC phases typically observed in amphiphile-water mixtures is shown in Fig. S5 below, as an ideal, symmetric phase diagram.[11] However, not all amphiphile-solvent systems show all of these phases, and actual phase diagrams are generally not this symmetric in nature.

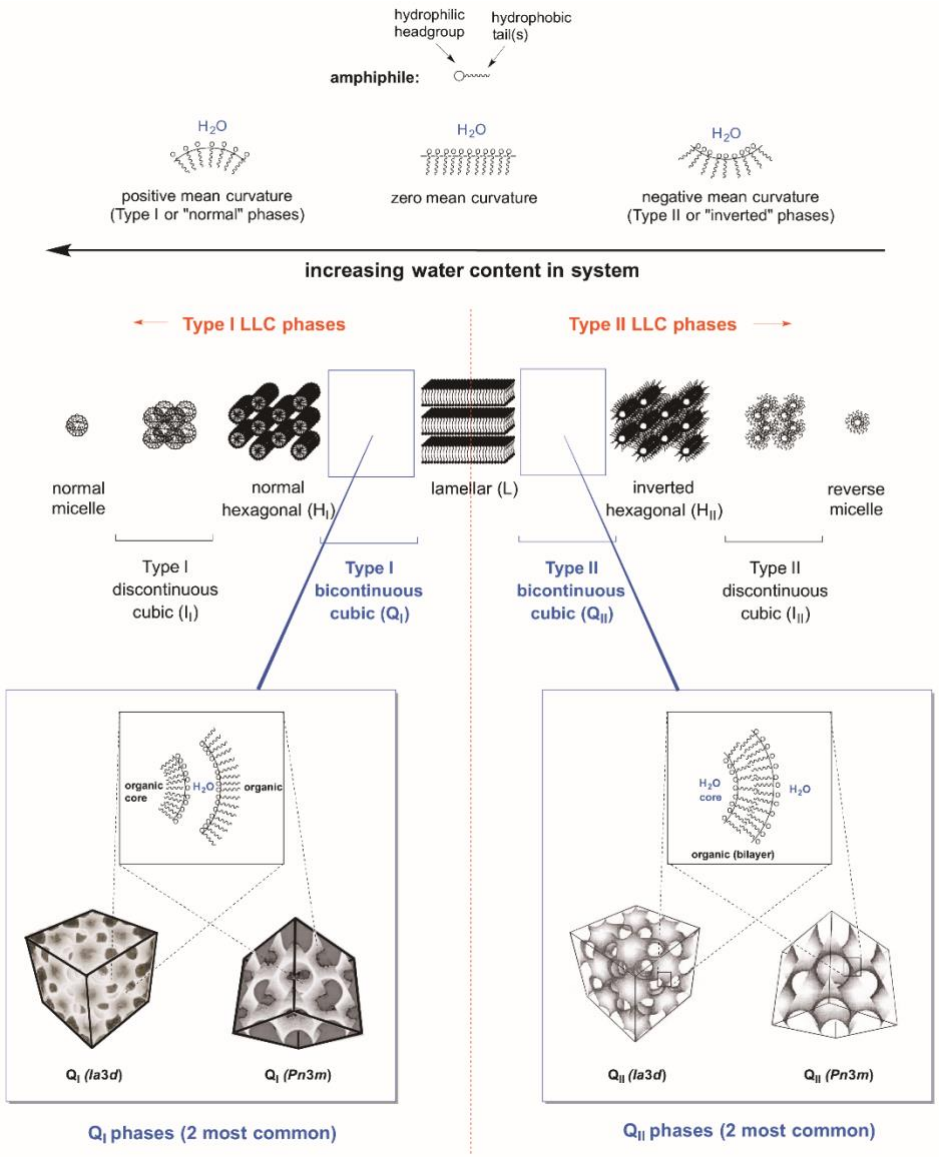

Fig. S5 Schematic representations of the most common LLC phases formed by amphiphiles in water in an ideal phase progression, with a focus on the Q phases. Partially reproduced from Ref. 11 with permission. Copyright Nature Publishing Group, 2012.

Assignment of LLC phase regions was done by first assessing if the PLM optical texture was black or birefringent. If the optical texture was black and the corresponding PXRD spectrum

had a broad/weak principal peak or effectively no sharp diffraction peaks (see Fig. S16a), then the phase region was categorized as an amorphous isotropic phase (Iso) (i.e., an amorphous melt or unordered collection of normal or reverse spherical micelles). If the PLM optical texture was birefringent and the PXRD spectrum exhibited a single or multiple sharp diffraction peaks, then the observed phase was assigned as hexagonal (H), lamellar (L), or an unidentified anisotropic phase or mixture of unidentified anisotropic phases (Unidentified anisotropic phase(s)). H phases have PXRD peaks with a *d*-spacing pattern of 1: $1/\sqrt{3}$: $1/\sqrt{4}$: $1/\sqrt{7}$: $1/\sqrt{9}$…etc. with respect to the principal peak.[3, 10] L phases have PXRD peaks with a *d*-spacing pattern of 1: 1/2: 1/3: 1/4: 1/5…etc. with respect to the principal peak.[3, 10] If the PXRD spectrum showed *d*-spacings that could not be clearly indexed to those of H or L phases but the presence of a sharp peak or peaks suggested some degree of order, then the phase was assigned as an Unidentified anisotropic phase(s), depending if there were multiple sharp peaks in the spectrum.

Assignment of Q phase regions and discontinuous cubic phase regions (I) was done by confirming the presence of a black, pseudo-isotropic optical texture (as a consequence of their cubic symmetry) and differences in their PXRD order. I phases typically have PXRD peaks with a *d*-spacing ratio of 1: $1/\sqrt{3}$: $1/\sqrt{8}$: $1/\sqrt{11}$: $1/\sqrt{12}$,…etc, with respect to the principal peak.[12, 13] They are also typically optically transparent because of their cubic symmetry but are not very viscous because they consist of cubic-packed individual normal or reverse micelles with minimal contact with each other.[10, 12] In contrast, Q phases typically exhibit PXRD peaks with a *d*-spacing pattern of $1/\sqrt{6}$: $1/\sqrt{8}$: $1/\sqrt{20}$: $1/\sqrt{22}$,…etc. with respect to the principal peak.[3, 10] Q phases also are optically transparent but are typically very viscous in nature because they consist of 3D-interpenetrating hydrophobic and hydrophilic channel systems.[10] Based on these features and differences in features, phase regions that have black PLM optical textures and PXRD order could

be differentiated into Q and I phases. Weakly ordered Q phases were identified as Q phases that followed the appropriate *d*-spacing pattern but had a broader than usual principal peak.

In addition, each H, Q, or I phase with the specific geometry/symmetry described above can also be sub-classified in terms of whether the phase curves around the hydrophobic domains (i.e., normal / Type I) or around the hydrophilic domains (inverted / Type II).[10] To unequivocally determine whether an observed LLC phase is Type I or Type II, an L phase needs to be present in the phase diagram as a central reference point that has no preferred net curvature towards either the hydrophilic or hydrophobic domains. Then, LLC phases on the solvent-excessive side of the L phase can be assigned as Type I (normal), and those on the solvent-deficient side can be assigned as Type II (inverted).[10] Unfortunately, only one of the homologues studied in this work showed an L phase in its partial phase diagram (i.e., **[7H, 18T]** with water); none of the homologues that showed a Q phase (i.e., **[5H, 18T]**, **[9H, 18T]**, **[5H, 14T]**, and **[6H, 14T]**) also exhibited an identifiable L phase for a clear Type I vs. Type II phase assignment.

Using the combined PLM and PXRD data and criteria above, partial phase diagrams of the seven monomer **1** homologues were created as a function of system composition and temperature.

NMR spectra.

Included below are NMR spectra of several monomers demonstrating that for each homologue the chemical shifts remained consistent while the integration values of the alkyl regions changed.

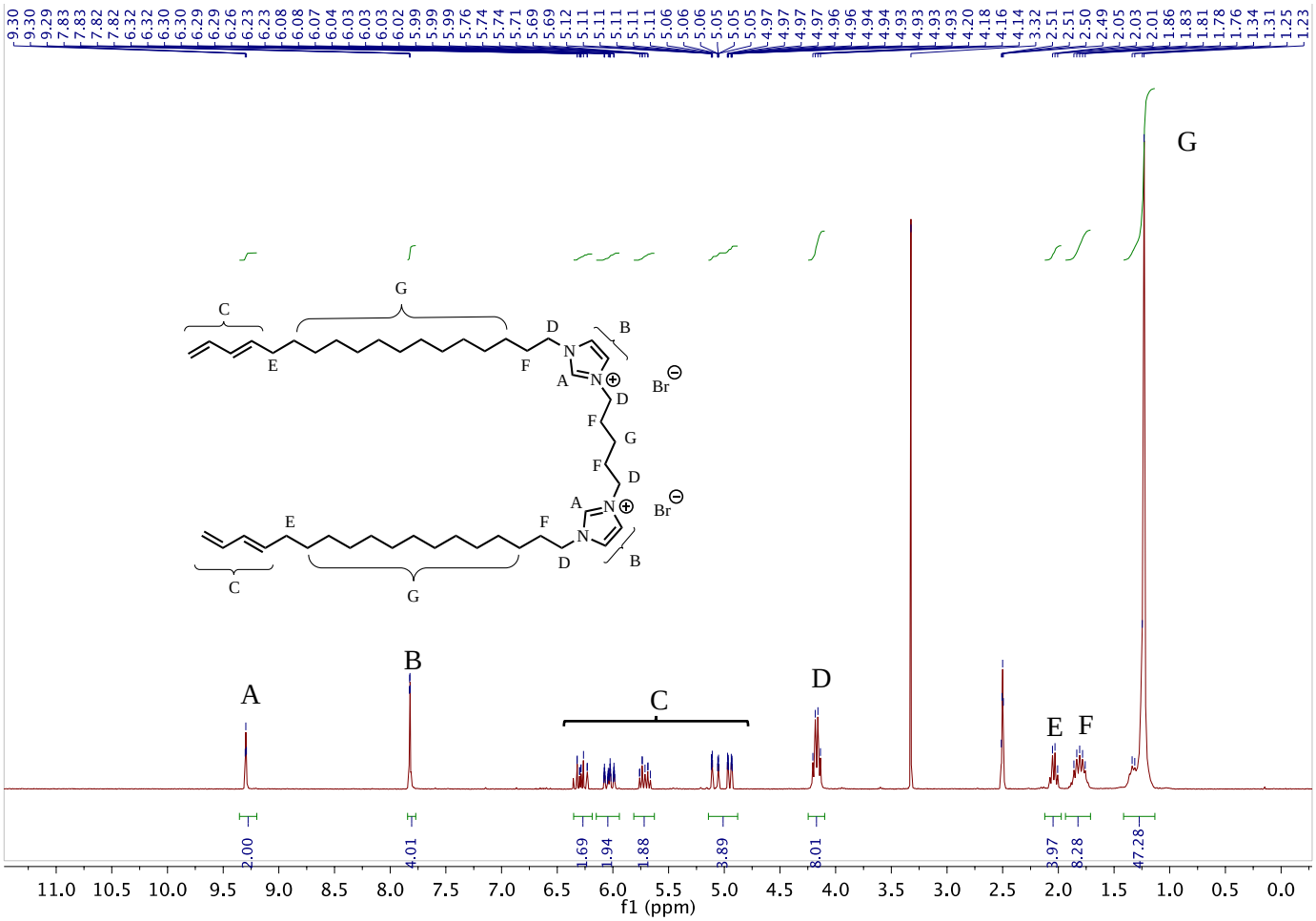

Fig. S6 ^{1}H NMR spectrum of **[5H, 18T]** in DMSO-*d*$_6$.

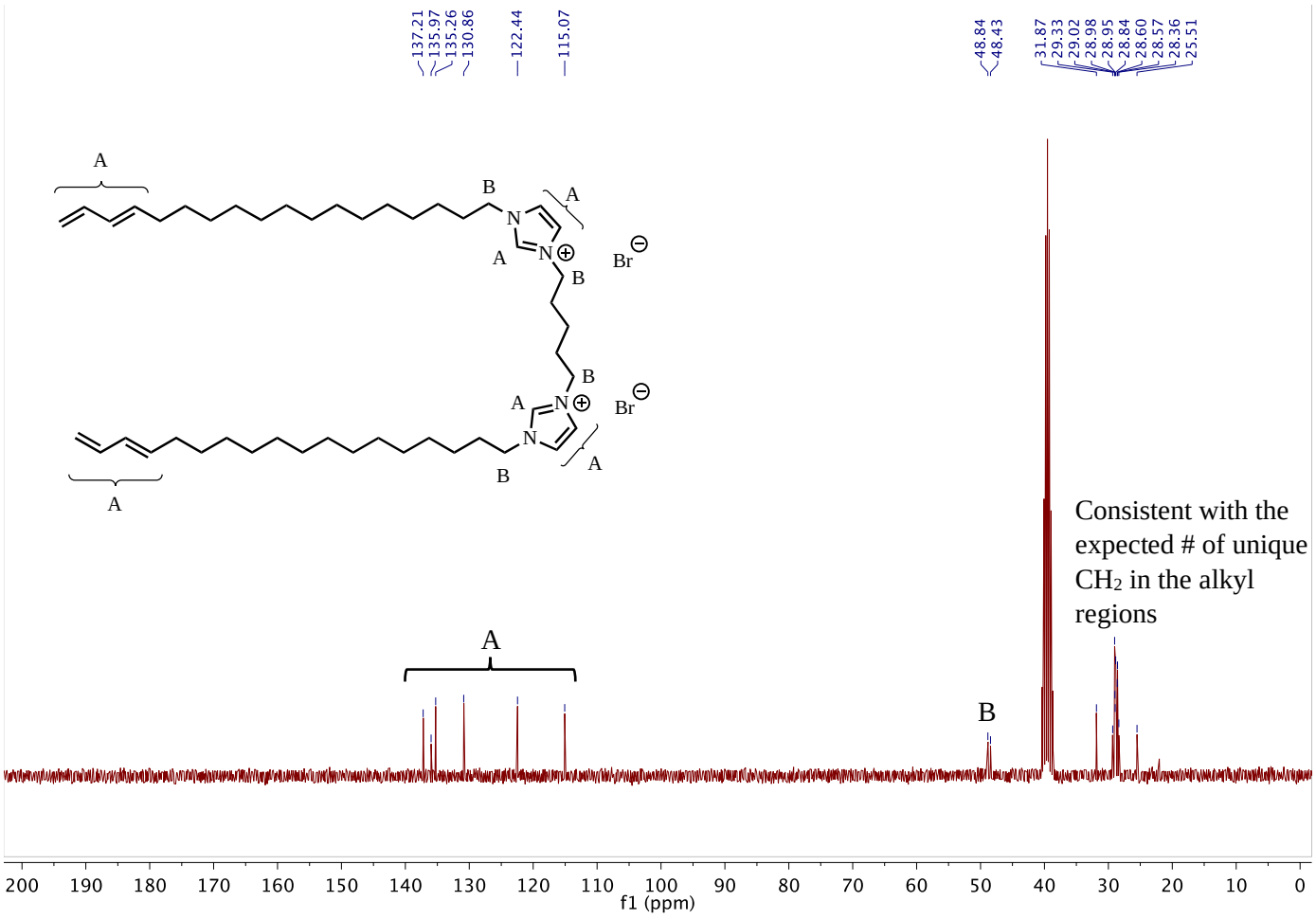

Fig. S7 ^{13}C NMR spectrum of **[5H, 18T]** in DMSO-*d*$_6$.

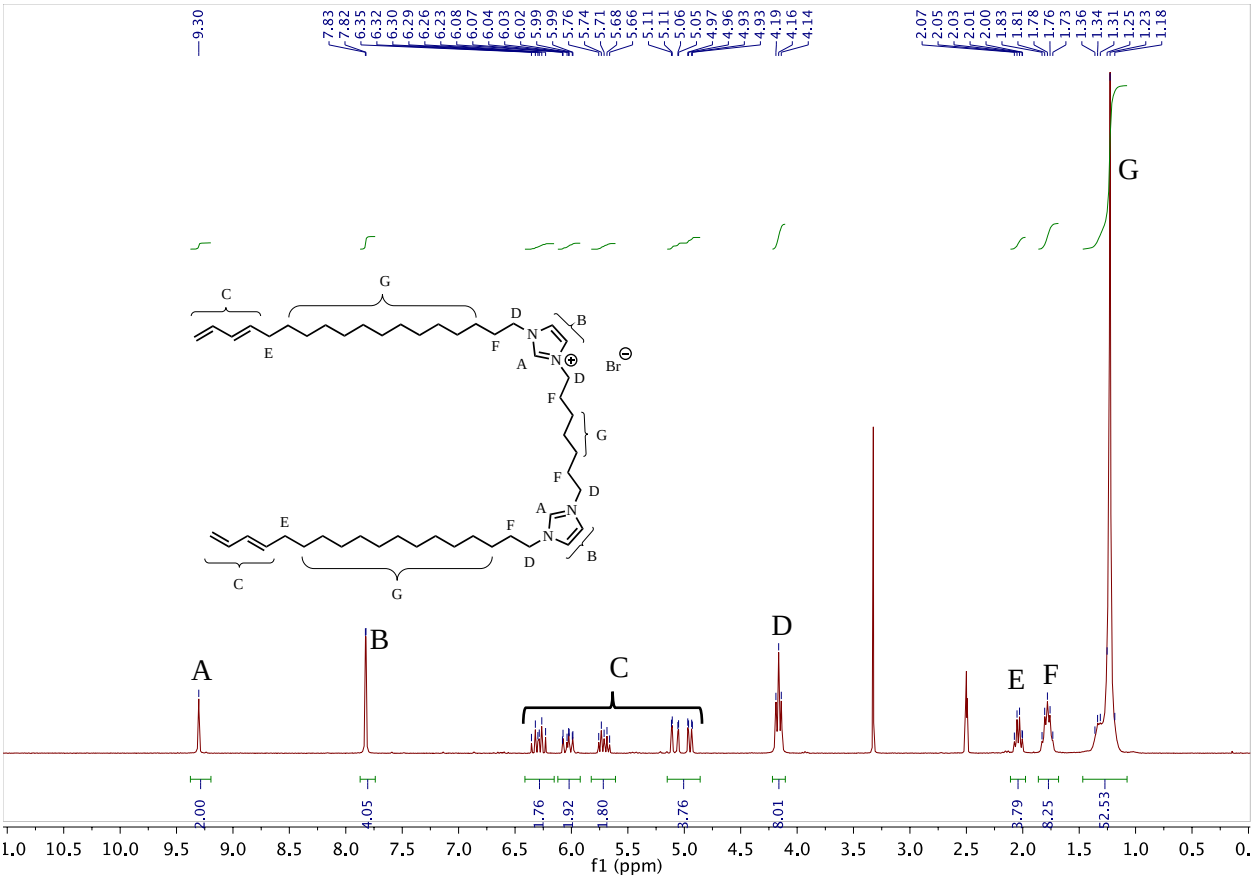

Fig. S8 ^{1}H NMR spectrum of **[7H, 18T]** in DMSO-*d*$_6$.

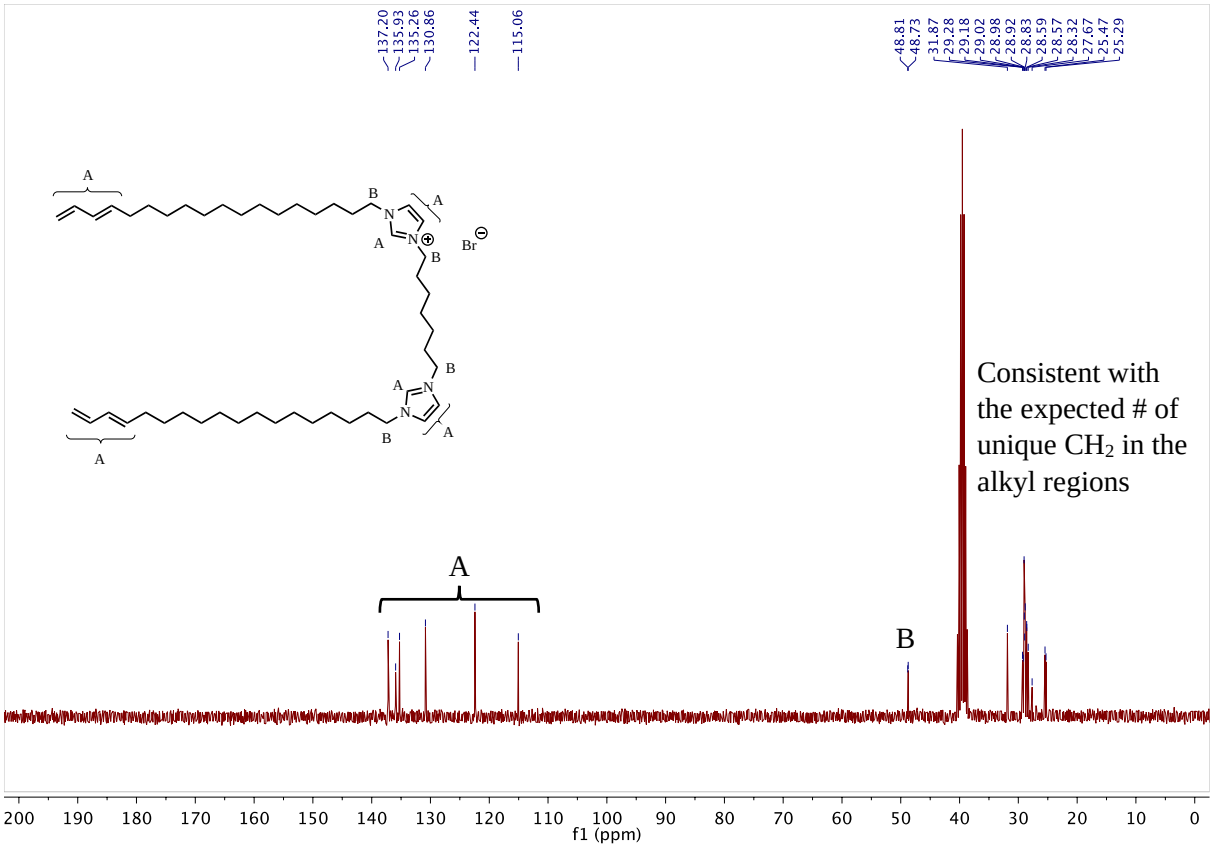

Fig. S9 ^{13}C NMR spectrum of **[7H, 18T]** in DMSO-d_6.

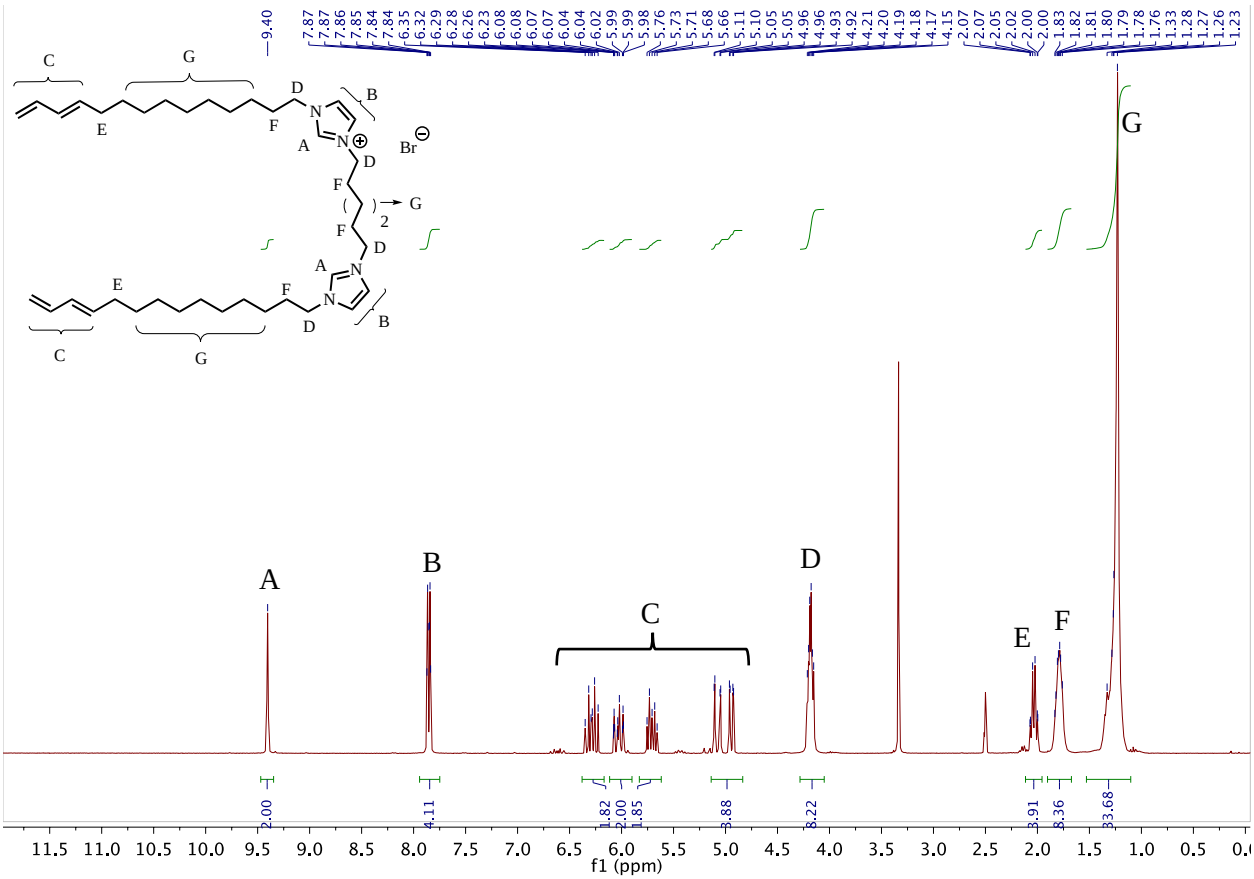

Fig. S10 ^{1}H NMR spectrum of **[6H, 14T]** in DMSO-d_6.

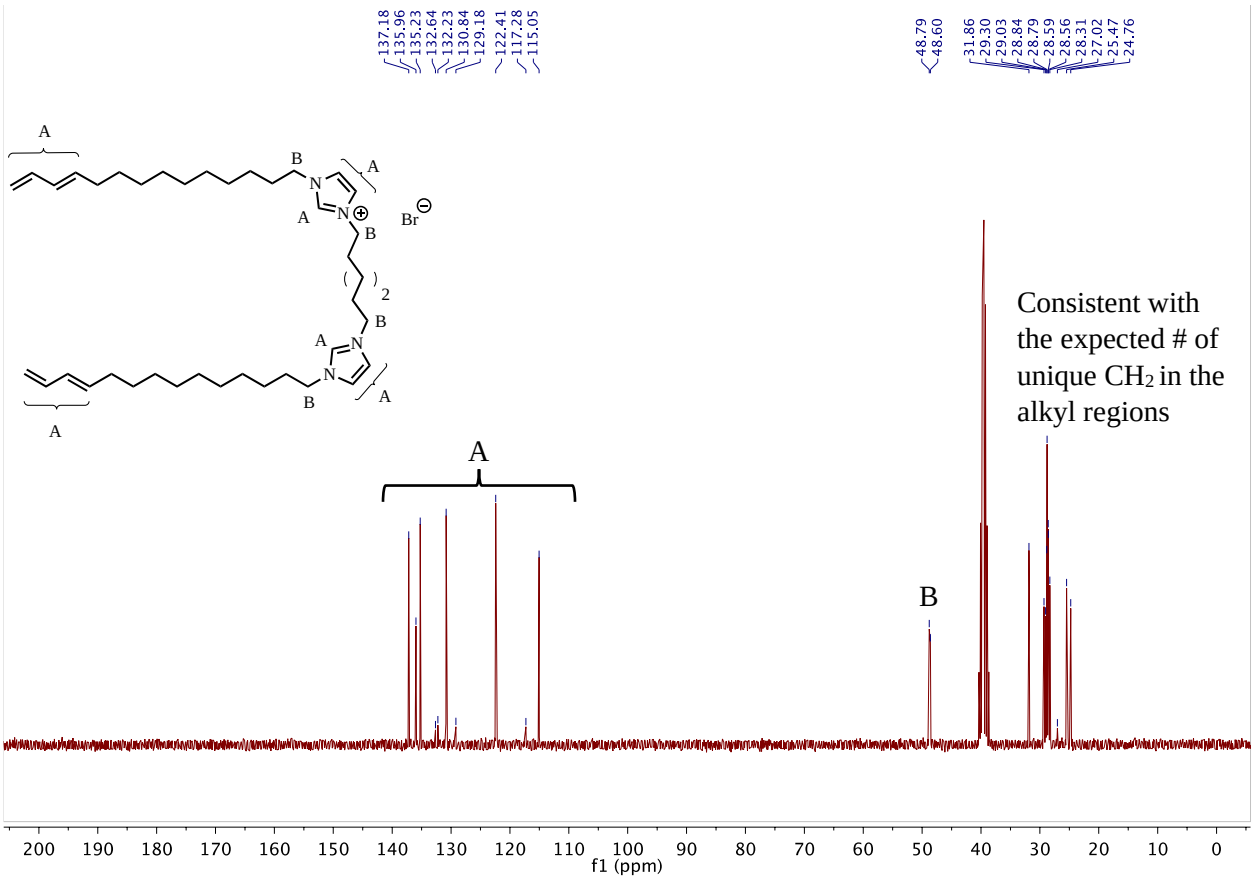

Fig. S11 ^{13}C NMR spectrum of **[6H, 14T]** in DMSO-d_6.

Homologue partial phase diagrams not shown in Fig. 2 in the main manuscript.

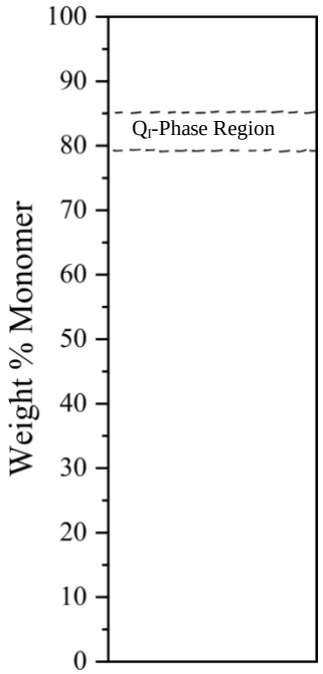

Fig. S12 Partial phase diagram of monomer **1** in glycerol at 65 °C constructed from data published in the Supp. Info. for Ref. 2.

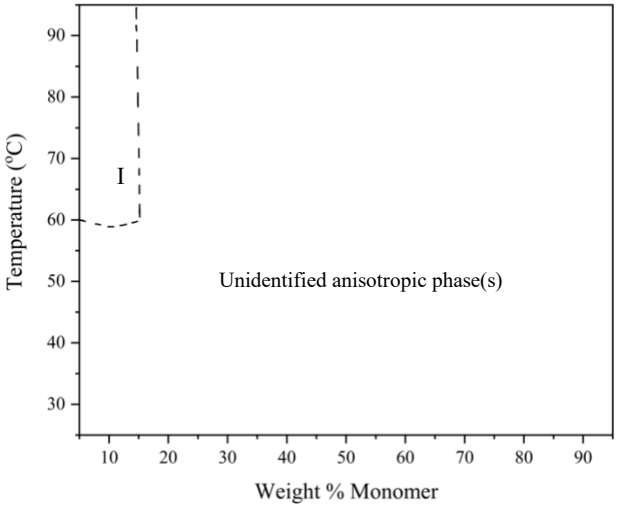

Fig. S13 Partial phase diagram of **[5H,18T]** with water. I = discontinuous cubic phase.

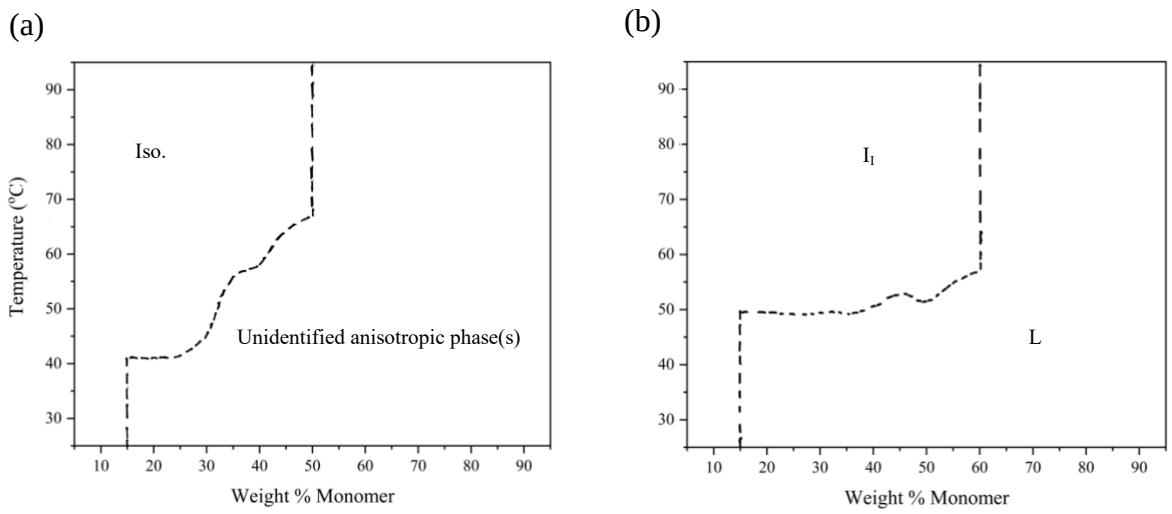

Fig. S14 Partial phase diagrams of **[7H, 18T]** with (a) glycerol and (b) with water. Iso. = amorphous isotropic phase; L = lamellar phase; I_I = Type I discontinuous cubic phase.

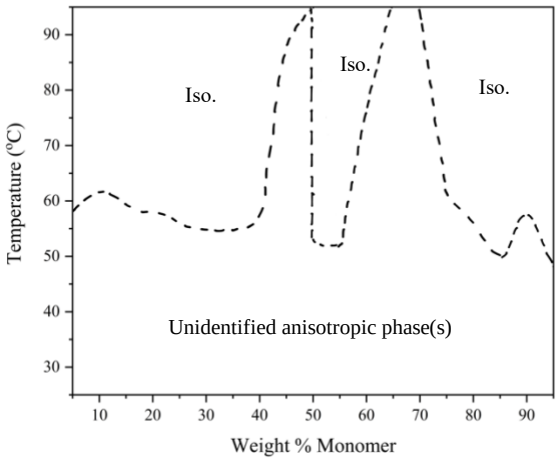

Fig. S15 Partial phase diagram of **[9H, 18T]** in water. Iso. = amorphous isotropic phase.

Note: Although **[4H, 14T]** in water demonstrated the potential to form a Q phase by preliminary PLM penetration scan analysis (Table S1), more detailed and careful PLM composition and temperature analysis revealed that **[4H, 14T]** with water did not display any completely black optical textures. The lack of a black optical texture during the detailed PLM analysis implied that a pure Q phase was not present and thus did not require further study via

PXRD analysis. We hypothesize that the lack of a Q phase for **[4H, 14T]** may potentially be related to the spacer length between the ionic headgroups. With shortening spacer lengths, the ionic interactions between the headgroups may become more pronounced and could affect the ability of a gemini amphiphile to form a particular phase.[14, 15]

For samples that demonstrated the potential to form a Q phase during preliminary PLM-based solvent-penetration scan screening (Table S1) and exhibited optically black regions during detailed PLM composition and temperature analysis, PXRD analysis was utilized to quantitatively confirm if the optically black region was a Q phase or a different type of optically isotropic phase. In some cases (e.g., **[5H, 14T]** in glycerol), rapid PLM penetration scan screening analysis suggested the potential for Q phase formation (Table S1), whereas the full PLM characterization followed by PXRD analysis of carefully prepared sample mixtures did not reveal formation of an actual Q phase (see Table 1 in the main manuscript).

Example PXRD profiles and PLM images used for phase assignments in the elucidation of the partial phase diagrams.

Note: It was not possible to identify whether the Q phases formed were *Ia3d* or *Pn3m* from the PXRD spectra in the main manuscript and ESI. Neither our PXRD instrument (nor our collaborator's SAXS instrument) was able to resolve enough diffraction peaks in the Q-phase samples to unequivocally identify an *Ia3d* or a *Pn3m* unit cell.

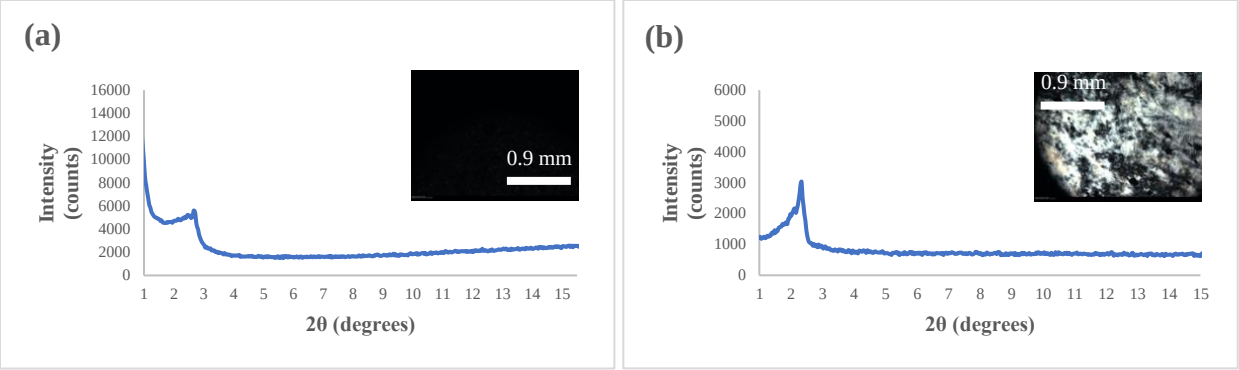

Fig. S16 Example PXRD profiles and PLM images used to assign disordered isotropic (Iso) phases and unidentified anisotropic phase(s) in the partial phase diagram: (a) VT-PXRD profile and PLM image of a disordered isotropic (Iso) phase obtained from an unpolymerized mixture of 30/70 (w/w) **[5H, 18T]**/glycerol at 65 °C. (b) PXRD profile and PLM image of an unidentified anisotropic phase or mixture of phases obtained from a mixture of 70/30 (w/w) **[5H, 18T]**/glycerol at 65 °C.

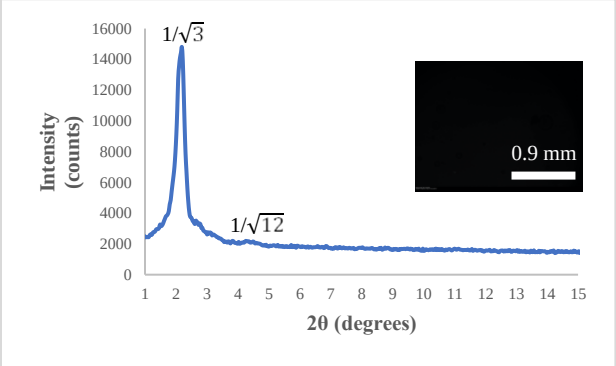

Fig. S17 VT-PXRD profile and PLM image of the discontinuous cubic (I) phase formed by an unpolymerized mixture of 10/90 (w/w) **[5H, 18T]**/water at 62 °C. The PXRD *d*-spacings and black optical texture are consistent with an I phase.[12, 13]

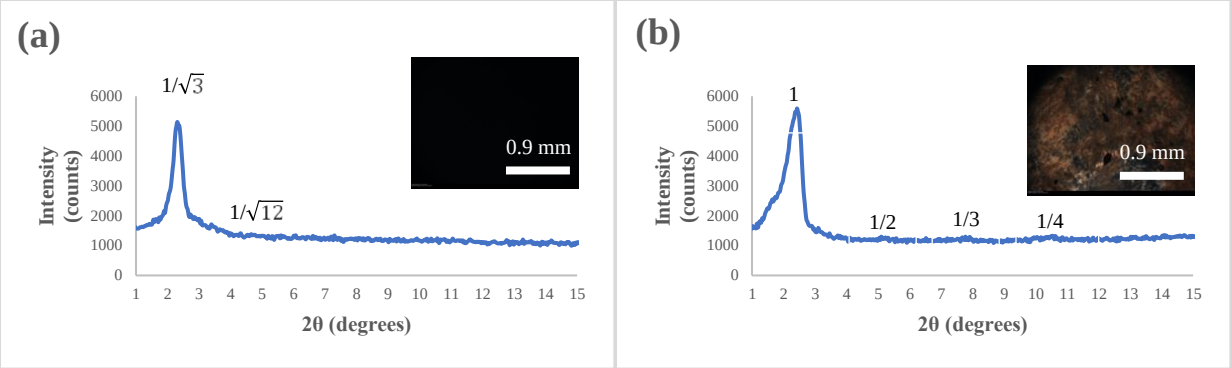

Fig. S18 Example VT-PXRD and PLM images of some LLC phases formed by **[7H, 18T]** with water: (a) VT-PXRD profile and PLM image of a discontinuous cubic (I) phase formed by an unpolymerized mixture of 40/60 (w/w) **[7H, 18T]**/water at 80 °C. The PXRD peak *d*-spacings and black optical texture consistent with an I phase.[12, 13] (b) VT-PXRD profile and PLM image of the lamellar (L) phase formed by an unpolymerized mixture of 75/25 (w/w) **[7H, 18T]**/water at 50 °C. The equally spaced 2θ peaks and birefringent optical texture are indicative of an L phase.[3, 10]

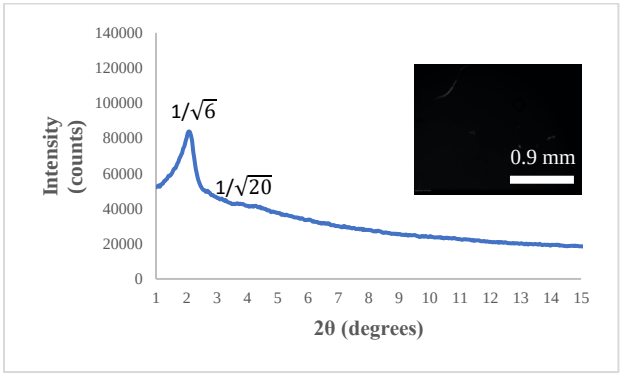

Fig. S19 PXRD profile and PLM image of a bulk cross-linked Q-phase film formed by photopolymerization of a mixture of 74/25/1 (w/w/w) **[9H, 18T]**/glycerol/HMP at 55 °C.

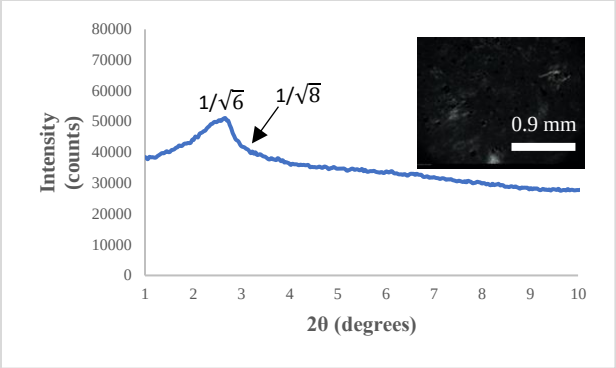

Fig. S20 PXRD profile and PLM image of a bulk cross-linked Q-phase film formed by photopolymerization of a mixture of 89/10/1 (w/w/w) **[5H, 14T]**/water/HMP at 55 °C.

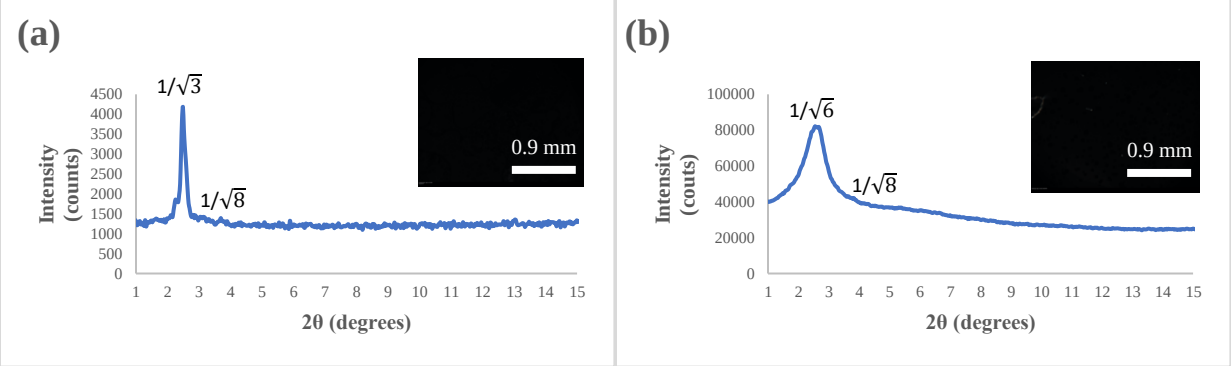

Fig. S21 Example PXRD and PLM images of some LLC phases formed by **[6H, 14T]** with water: (a) VT-PXRD profile and PLM image of a discontinuous cubic (I) phase formed by an unpolymerized mixture of 10/90 (w/w) **[6H, 14T]**/water at 30 °C. The PXRD peak *d*-spacings and black optical texture consistent with an I phase.[12, 13] (b) PXRD profile and PLM image of a bulk cross-linked Q-phase film formed by photopolymerization of a mixture of 84/15/1 (w/w/w) **[6H, 14T]**/water/HMP at 55 °C.

Single-run SAXS profile obtained to confirm the Q-phase structure of a cross-linked sample analyzed by PXRD.

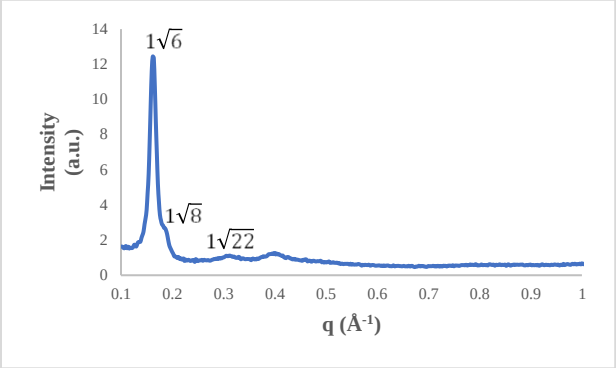

Fig. S22 SAXS profile of a bulk cross-linked Q-phase film prepared from a mixture of **[5H, 18T]**/glycerol/HMP (79:20:1 (w/w/w)) for which a PXRD spectrum was shown in Fig. 2 in the main manuscript. The signal at ca. 0.4 $Å^{-1}$ is from Kapton film support.

As can be seen from the SAXS spectrum above, the primary peak and shoulder appear to be in a ratio of $1/\sqrt{6} : 1/\sqrt{8}$. Both the PXRD and SAXS profiles for this sample are consistent with one another and indicative of a Q phase. However, given the lack of other discernable peaks, we refrain from assigning a specific space group to the Q phase of this sample (and similarly to the other observed Q phases in this manuscript).

Example FT-IR data for determining the extent of polymerization in photo-cross-linked Q-phase samples.

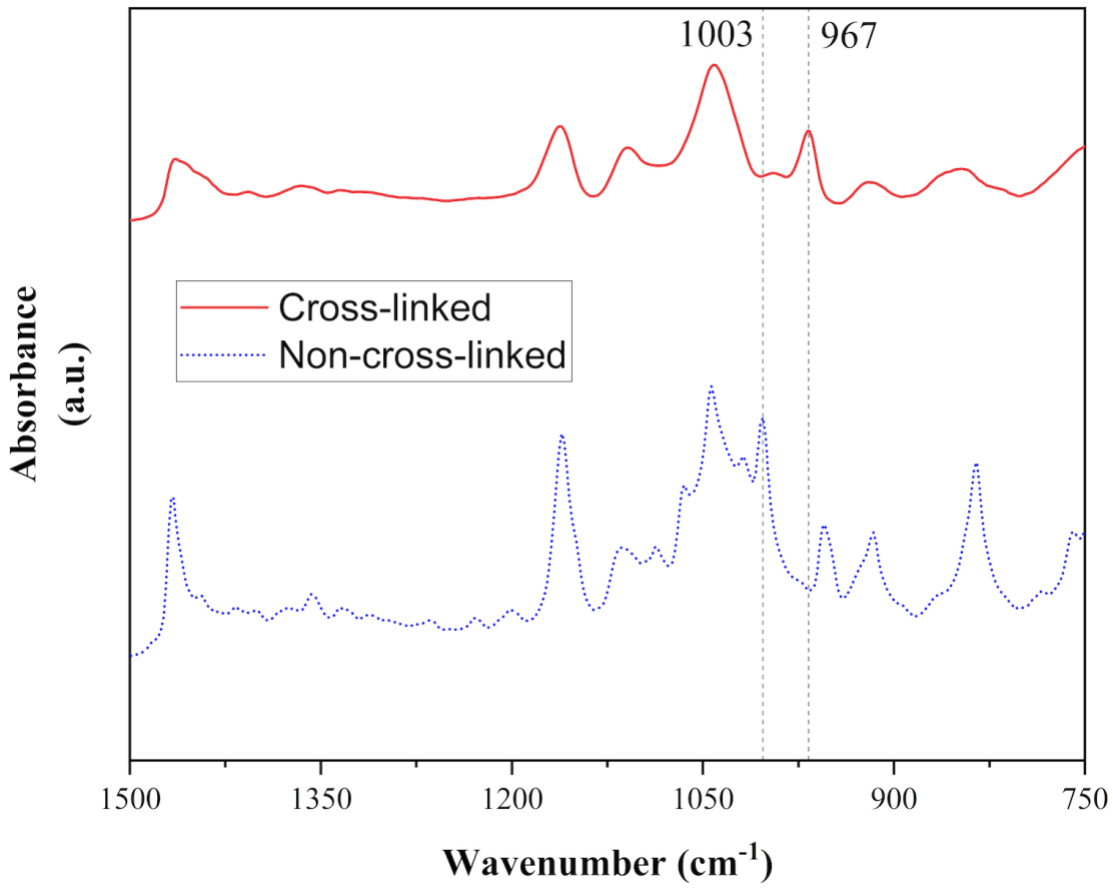

Fig. S23 Representative FT-IR spectra of a bulk Q-phase film of a mixture of 79/20/1 (w/w/w) **[5H, 18T]**/glycerol/HMP pre- and post-photopolymerization. The disappearance of the band at 1003 cm^{-1} (corresponding to the -C–H out-of-plane wag of CH_2=CH_2) and the appearance of a new band at 967 cm^{-1} (corresponding to CH=CH *trans* units) signify essentially complete 1,3-diene group conversion.[16]

References for the ESI

1. T. N. Blanton, T. C. Huang, H. Toraya, C. R. Hubbard, S. B. Robie, D. Louër, H. E. Göbel, G. Will, R. Gilles and T. Raftery, *Powd. Diffract*. 1995, **10**, 91.
2. B. M. Carter, B. R. Wiesenauer, E. S. Hatakeyama, J. L. Barton, R. D. Noble and D. L. Gin, *Chem. Mater*. 2012, **24**, 4005.
3. B. A. Pindzola, J. Jin and D. L. Gin, *J. Am. Chem. Soc.* 2003, **125**, 2940.
4. B. A. Pindzola, B. P. Hoag and D. L. Gin, *J. Am. Chem. Soc.* 2001, **123**, 4617.
5. G. Piancatelli, *Encyclopedia of Reagents for Organic Synthesis*, 2001, 1, John Wiley & Son Ltd., United Kingdom.
6. B. P. Hoag and D. L. Gin, *Macromolecules* 2000, **33**, 8549.
7. S. Sharma, M. Tandon and J. W. Lown, *J. Org. Chem.* 2000, **65**, 1102.
8. J. E. Bara, E. S. Hatakeyama, B. R. Wiesenauer, X. Zeng, R. D. Noble and D. L. Gin, *Liq. Cryst.* 2010, **37**, 1587.
9. I. Merino, J. D. Thompson, C. B. Millard, J. J. Schmidt and Y-P. Pang, *Bioorg. Med. Chem.* 2006, **14**, 3583.
10. For general reviews on LLC phases and their classifications, see: (a) Tate, M. W.; Eikenberry, E. F.; Turner, D. C.; Shyamsunder, E.; Gruner, S. M. *Chem. Phys. Lipids* 1991, **57**, 147. (b) Seddon, J. M. *Biochim. Biophys. Acta* 1990, **1031**, 1. (c) Tiddy, G. J. T. *Phys. Rep.* 1980, **57**, 1.
11. B. R. Wiesenauer and D. L. Gin, *Polym. J.*, 2012, **44**, 461.
12. J. M. Seddon, J. Robins, T. Gulik-Krzywicki and H. Delacroix, *Phys. Chem. Chem. Phys.* 2000, **2**, 4485.
13. Y. Huang and S. Gui, *RSC Adv.* 2018, **8**, 6978.

14. D. V. Perroni, C. M. Baez-Cotto, G. P. Sorenson and M. K. Mahanthappa, *J. Phys. Chem. Lett.* 2015, **6**, 993.

15. S. Mantha, J. G. McDaniel, D. V. Perroni, M. K. Mahanthappa and A. Yethiraj, *J. Phys. Chem. B.* 2017, **121**, 565.

16. M. Zhou, P. R. Nemade, X. Lu, X. Zeng, E. S. Hatakeyama, R. D. Noble and D. L. Gin, *J. Am. Chem. Soc.* 2007, **129**, 9574.